

Simple Solid State Synthesis of Nanostructured $\text{Ag}_6\text{Mo}_{10}\text{O}_{33}$ and Ni-Substituted $\text{Ag}_6\text{Mo}_{10}\text{O}_{33}$ Polyoxometalates with Photocatalytic Characteristic

A. Tadjarodi^{1*}, M. Imani¹ and A. Irajizad²

* tajarodi@iust.ac.ir

Received: June 2017

Accepted: April 2017

¹ Research Laboratory of Inorganic Materials Synthesis, Department of Chemistry, Iran University of Science and Technology, Tehran, Iran.

² Department of Physics, Sharif University of Technology, Tehran, Iran.

² Institute for Nanoscience and Nanotechnology (INST), Sharif University of Technology, Tehran Iran.

DOI: 10.22068/ijmse.14.3.48

Abstract: In this work, we report the synthesis of silver decamolybdate, $\text{Ag}_6\text{Mo}_{10}\text{O}_{33}$, nanostructure by a simple mechanochemical process followed by calcination treatment using acetamide as driving agent. Morphological study by scanning electron microscopy (SEM) images revealed bundles of rods grown closely together with an average diameter of 92 nm for $\text{Ag}_6\text{Mo}_{10}\text{O}_{33}$ sample. Ni-substituted $\text{Ag}_6\text{Mo}_{10}\text{O}_{33}$ compound was prepared via introducing nickel cation to precursor system in mechanical milling step. The particle size decreased to 87 nm by incorporating nickel units in substituted polymolybdate. It was concluded that the suitable selection of reagents can direct solid phase reaction towards producing nanostructured products. This technique is easy and simple for preparation of various mixed metal oxides without using any solvents and or complex procedures. In addition, the photocatalytic activity of the prepared products was studied on the removal of 4-nitro phenol (4-NP) as organic pollutant from water. The obtained results were also discussed in detail.

Keywords: Mechanochemical Reaction, Polyoxometalate, Nanostructure, Photocatalytic Characteristic.

1. INTRODUCTION

In recent years, metal polymolybdates as a category of mixed metal oxides have aroused most attentions of researches due to their effective applications in gas sensors, photocatalysts, optical and electrical devices, etc [1-3]. Amongst these compounds, silver polymolybdates such as $\text{Ag}_2\text{Mo}_2\text{O}_7$, $\text{Ag}_2\text{Mo}_4\text{O}_{13}$, $\text{Ag}_2\text{Mo}_3\text{O}_{10}$ and $\text{Ag}_6\text{Mo}_{10}\text{O}_{33}$ are more considerable in conducting glasses, catalysts and gas sensing applications because of the special chemical and physical properties [2, 4-6]. On the other hands, the synthesis of nanomaterials by new and simple strategies in large amounts became an important task due to the increase of their demand and applications in different scientific and industrial branches. Up to now, several methods have been introduced to synthesize the different phases of silver polymolybdates. Solution approaches are the most common methods reported for the synthesis of nano-sized silver polymolybdates. Although there are reports in literature about the synthesis

of these materials, the most common methods in preparation of these oxides, especially $\text{Ag}_6\text{Mo}_{10}\text{O}_{33}$, include the severe reactions between molybdenum trioxide and silver oxide under high heating temperature for long times and or harsh pH conditions [5-8]. Based on the reported works, silver decamolybdate is not presented as a stable phase compared with the other kind of silver polymolybdates, which limits the preparation of this product. Although the synthesis of a wide spectrum of nanomaterials has been reported by mechanochemical reaction, there is no report on the production of $\text{Ag}_6\text{Mo}_{10}\text{O}_{33}$ rod-like nanostructure and also, Ni-substituted one by utilizing this process. In fact, mechanochemical process using proper reagents can be introduced as a simple technique to prepare $\text{Ag}_6\text{Mo}_{10}\text{O}_{33}$ and or other polymolybdates in nanoscale. Likewise, this method is performed in solid phase without using any organic solvents and therefore, it is an environmentally friendly method.

Since the presence of wastes in water bodies and their long-term toxic effects are the serious

threats for organisms and human, study on the photocatalytic performance of different materials can open new pathways for dealing with such problems. In this work, we report the synthesis of rod-like nanostructures of $\text{Ag}_6\text{Mo}_{10}\text{O}_{33}$ and Ni-substituted $\text{Ag}_6\text{Mo}_{10}\text{O}_{33}$ by mechanochemical reaction followed by heat treatment in latter low temperature. Then, the photocatalytic behavior of Ni-substituted product was studied for removal of 4-nitro phenol (initial concentration of 10 mg. L⁻¹) as a model of organic pollutant in water.

2. EXPERIMENTAL

2. 1. Materials and Synthesis Procedure

All chemicals were purchased from Merck Co. and were used without further purification.

To prepare $\text{Ag}_6\text{Mo}_{10}\text{O}_{33}$ nanostructure, the stoichiometric amounts of $(\text{NH}_4)_6\text{Mo}_7\text{O}_{24}\cdot 4\text{H}_2\text{O}$ and AgNO_3 as starting materials in the presence of acetamide/ammonium nitrate as driving /oxidizer agent (molar ratio of 2:1) were milled in solid phase in a ball milling apparatus (Retsch MM-400, Germany) with a rate of 1800 rpm for 60 min. The resultant pasty precursor was collected and treated at 450 °C for 2 h and then, the obtained pale yellow powder was characterized.

The Ni-substituted $\text{Ag}_6\text{Mo}_{10}\text{O}_{33}$ sample was synthesized via running similar reaction in the presence of desired amount of nickel metal source (nickel nitrate hexahydrate, $\text{Ni}(\text{NO}_3)_2\cdot 6\text{H}_2\text{O}$).

To study the photocatalytic activity of the Ni-substituted sample, 50 mL aqueous solution of 4-nitrophenol (4-NP) with a initial concentration of 10 mg L⁻¹ was treated in the presence of 0.02 g of this sample for 150 min under light irradiation. The visible irradiation was supplied by using a source of 500 W high-pressure mercury-vapor lamp ($\lambda = 546.8 \text{ nm}$).

2. 2. Characterizations

The X-ray diffraction (XRD) patterns were recorded by a STOE powder diffraction system using $\text{Cu K}\alpha$ radiation (wavelength, $\lambda = 1.54060 \text{ \AA}$). Fourier transform infrared (FT-IR) spectra were recorded on a Shimadzu-8400S

spectrometer in the range of 400–4000 cm^{-1} using KBr pellets. Scanning electron microscopy (SEM) images and energy-dispersive X-ray spectroscopy analysis (EDX) were taken on VEGA\TESCAN S360 with gold coating. Elemental analysis was performed by ICP analysis on sequential plasma spectrometer, Shimadzu (ICPS-7000 ver. 2). Diffuse-reflectance spectrum (DRS) was prepared via a Shimadzu (MPC-2200) spectrophotometer. The UV-Vis absorption studies were performed in the wavelength range of the 190–800 nm on a UV-Vis spectrometer (ShimadzuUV-1700).

3. RESULTS AND DISCUSSION

XRD patterns of the prepared products shown in Fig. 1 reveal the formation of a pure phase of silver decamolybdate, $\text{Ag}_6\text{Mo}_{10}\text{O}_{33}$ with similar pattern. The recorded diffraction peaks are in a close agreement with triclinic phase of $\text{Ag}_6\text{Mo}_{10}\text{O}_{33}$ and space group of $P\bar{1}$, $a = 7.59 \text{ \AA}$, $b = 8.31 \text{ \AA}$, $c = 11.42 \text{ \AA}$, $\alpha = 82.6^\circ$, $\beta = 102.9^\circ$ and $\gamma = 106.4^\circ$ (JCPDS Card No. 72-1689). The XRD pattern of Ni-substituted sample (Fig. 1b) shows a slight shift of the center of diffraction peaks toward higher angle compared to unsubstituted $\text{Ag}_6\text{Mo}_{10}\text{O}_{33}$ (e.g., in the inset of Fig. 1 is shown the slight shift of peak in 2θ position of 27.38 to 27.43°). This shift of peaks can be originated from the compaction of the crystalline unit cell due to the smaller ionic radius of incorporated nickel compared to Ag ion. FT-IR spectrum of the prepared precursor after milling process presented in Fig. 2a clearly shows the presence of organic functional groups. The observed broad peaks at $3000\text{--}3415 \text{ cm}^{-1}$ are specified as NH stretching vibration overlapped with O–H vibration band of H_2O molecules. The strong peaks are seen at 1656 and 1379 cm^{-1} , which can be related to CO and CN vibration frequencies of acetamide unit coordinated to metal center from carbonyl head. These bands can be probably overlapped with the vibration of ammonium and nitrate units. The C–H stretching vibration of the coordinated acetamide group is weakly seen at 2830 cm^{-1} because of overlapping with OH and NH stretching vibrations. The vibration band at the position of 1035 cm^{-1} is

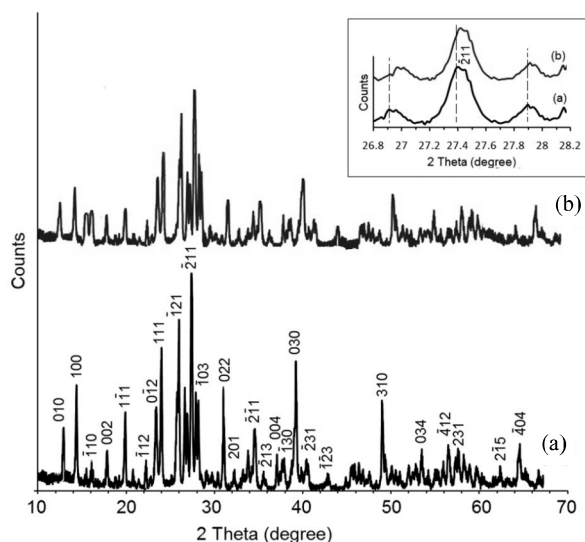


Fig. 1. XRD patterns of the prepared $\text{Ag}_6\text{Mo}_{10}\text{O}_{33}$ (a) and Ni-substituted $\text{Ag}_6\text{Mo}_{10}\text{O}_{33}$ (b).

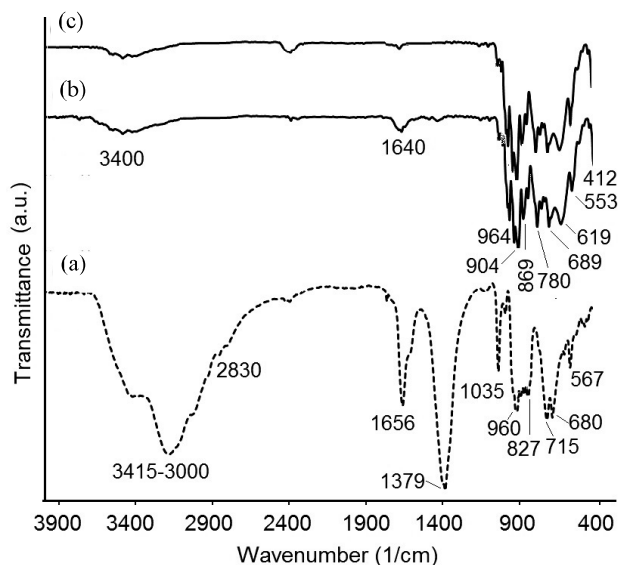


Fig. 2. FT-IR spectra of the precursor (a) the products after calcinations; $\text{Ag}_6\text{Mo}_{10}\text{O}_{33}$ (b) and Ni-substituted $\text{Ag}_6\text{Mo}_{10}\text{O}_{33}$ (c).

assigned to C-O of precursor structure. The characteristics bands at the range of 400-1000 cm^{-1} are related to metal-oxygen vibrations in precursor structure that are overlapped with bending vibrations of carbonyl and nitrate units

of this composition [9, 10]. Due to heat treatment, the organic functional groups were removed and only remained the vibration bands of polymolybdate oxide. The appeared peaks at the frequencies of 964, 904, 869, 780, 689, 619,

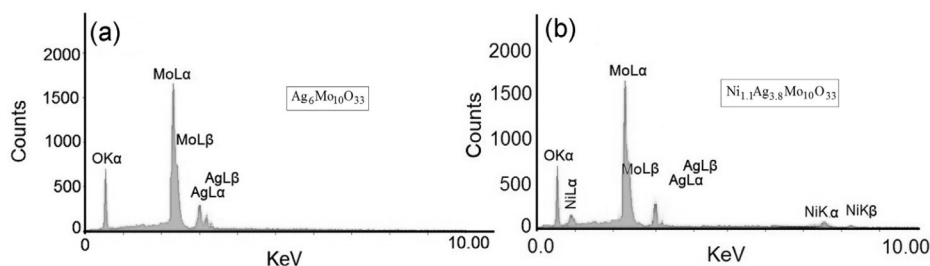


Fig. 3. EDX elemental analysis of the obtained $\text{Ag}_6\text{Mo}_{10}\text{O}_{33}$ (a) and Ni-substituted sample (b).

553 cm^{-1} in the product FT-IR spectrum (shown in Fig. 2b) belong to the stretching and bending vibrations of $\text{Mo}=\text{O}$, $\text{Mo}-\text{O}$, $\text{Mo}-\text{O}-\text{Mo}$ and $\text{O}-\text{Mo}-\text{O}$ as unshared, corner-shared and edge-shared oxygen of MoO_6 octahedral units in chains and bridging units of the prepared polymolybdate structure [10]. The peak at 412 cm^{-1} can be related to the characteristic band of silver-oxygen present in the prepared compound. The weak peaks also are visible at 1640 and 3400 cm^{-1} , which are assigned to the vibrations of the adsorbed H_2O molecules [9]. FT-IR spectrum of Ni-substituted sample is similar to un-substituted one (Fig. 2c). The XRD and FT-IR data confirm the formation of silver decamolybdate and Ni-substituted one.

Elemental analysis by EDX (Fig. 3a and b) and ICP demonstrated the presence of Ag, Mo and Ni elements in the prepared products. Based on the obtained percentages of 20.56 and 3.23 % for Ag^+ and Ni^{2+} by EDX and ICP analyses for the substituted sample, the formula of this product is determined as $\text{Ni}_{1.1}\text{Ag}_{3.8}\text{Mo}_{10}\text{O}_{33}$.

The SEM images of the prepared $\text{Ag}_6\text{Mo}_{10}\text{O}_{33}$ (Figs. 4a and b) display a bundle of rods that have grown close to each other with an average diameter of 92 nm and several micrometer sizes in length. It was found that the partial incorporation of nickel ions in system leads to the decrease of particle size to 87 nm, which can be expected due to the smaller ionic radius of nickel compared with Ag ion (Fig. 4c and d). We proposed the role of acetamide agent in formation of nanostructured materials in solid phase in our previous work [11]. Similarity, it is concluded that the use of acetamide/ammonium nitrate

agent has a key role in construction of building blocks of this structure. In fact, it is assumed that the high energy ball milling process leads to the coordination of acetamide to the metal centers by their functional groups accompanied by other present groups e.g. nitrate and or H_2O units. In fact, high energy mechanochemical reaction makes a large contact area of reactants and a highly dispersed phase of species. The prepared intermediate molecules called as precursor can easily transform to metal oxide form by heating

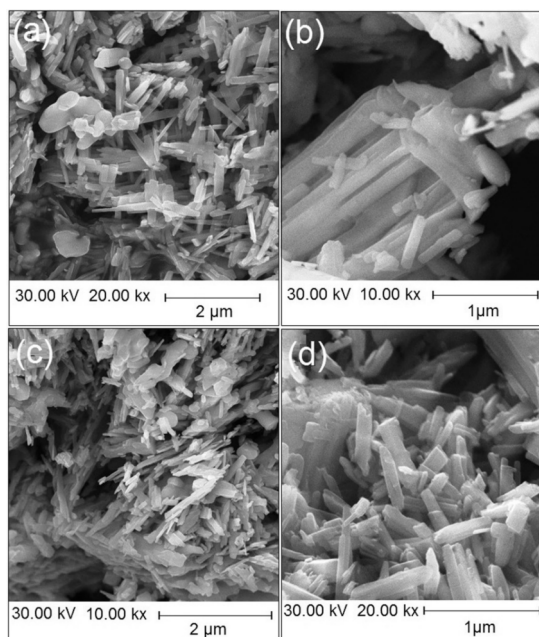


Fig. 4. SEM images of $\text{Ag}_6\text{Mo}_{10}\text{O}_{33}$ (a, b) and the Ni-substituted product (c, d).

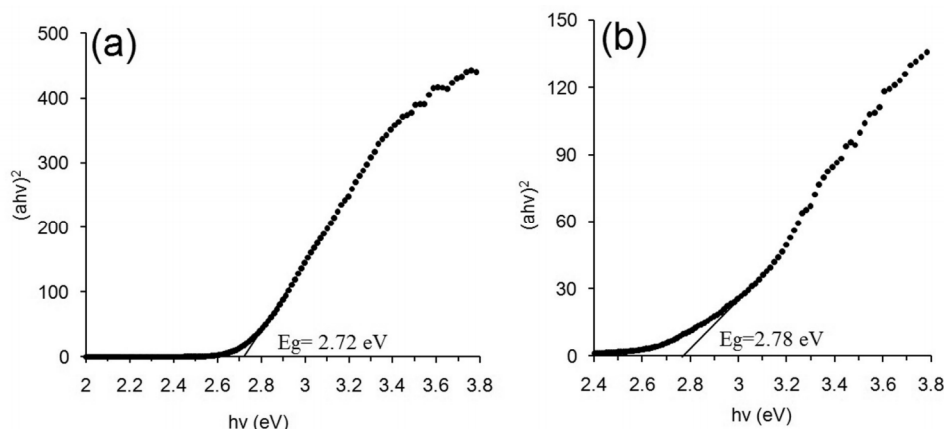


Fig. 5. The plots of $(\alpha hv)^2$ vs. $h\nu$ (eV) for $\text{Ag}_6\text{Mo}_{10}\text{O}_{33}$ (a) and Ni-substituted product (b).

decomposition of organic species and effectively growth of the nuclei sideways.

Band gap energies (E_g) of the prepared products optimal product were determined using Tauc equation (Eq. 1) obtained from Diffuse-reflectance spectra (DRS):

$$(\alpha hv)^2 = B(h\nu - E_g) \quad (1)$$

where, $h\nu$ is the photon energy, α is the

absorption coefficient, B is a constant value and E_g represents the band gap energy. By plotting the $(\alpha hv)^2$ vs. $h\nu$ in eV and obtaining the extrapolation points of these curves (Fig. 5), the band gap energies of the prepared $\text{Ag}_6\text{Mo}_{10}\text{O}_{33}$ and Ni-substituted one were estimated about 2.72 and 2.78 eV, respectively. These results reveal that these products can be a suitable candidate as a photocatalyst under visible light irradiation.

The study of the photocatalytic behavior of products was performed via monitoring the residual concentrations of 4-NP pollutant during 150 min illumination by UV-Vis spectroscopy. The removal efficiency of 93% (Fig. 6a) exhibits a high ability of Ni-substituted product compared with pristine $\text{Ag}_6\text{Mo}_{10}\text{O}_{33}$ (Fig. 6b) for photodegradation of 4-NP in water. A decrease of 35% of 4-NP concentration was observed after treatment in the dark (Fig. 6c), which is attributed to the adsorption of organic molecules on the surface of catalyst. A slight degradation of about 3% was observed for 4-NP under light irradiation without using any catalyst (Fig. 6d).

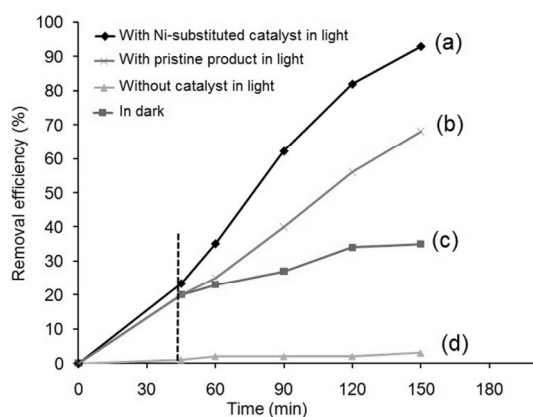


Fig. 6. Removal efficiency of 4-NP in water under light irradiation after 150 min using the prepared $\text{NiAg}_4\text{Mo}_{10}\text{O}_{33}$ (a), the prepared $\text{Ag}_6\text{Mo}_{10}\text{O}_{33}$ (b), in the dark (c) and without catalyst (d).

4. CONCLUSIONS

We performed a simple strategy to synthesize mixed metal oxide of silver decamolybdate and Ni-substituted one by selecting the proper reactants. The results showed the formation of the pure phase of $\text{Ag}_6\text{Mo}_{10}\text{O}_{33}$ with nanosized rod-

like morphology. In fact, the use of low-cost driving agent in the solvent-free mechanochemical reaction provides a particular substrate for the simple synthesis of nanomaterials. This method can be easily promoted to the large amount productions. The produced $\text{Ni}_{1.1}\text{Ag}_{3.8}\text{Mo}_{10}\text{O}_{33}$ showed a high photocatalytic activity for photodegradation of 4-NP in water revealing high capability of this product for photocatalytic treatments.

ACKNOWLEDGEMENTS

The financial support from Iran University of Science and Technology (IUST), Sharif University of Technology and Nanotechnology Initiative Council is gratefully acknowledged.

REFERENCES

1. Gupta, S. K., Ghosh, P. S., Sudarshan, K., Ruma, G., Pujari, P. K., Kadam, R. M., "Multifunctional pure and Eu^{3+} doped $\beta\text{-Ag}_2\text{MoO}_4$: photoluminescence", energy transfer dynamics and defect induced properties. Dalton. Trans., 2015, 44, 19097-19110.
2. Feng, M., Zhang, M., Song, J. M., Li, X. G. and Yu, S. H., "Ultralong Silver Trimolybdate Nanowires: Synthesis, Phase Transformation, Stability, and Their Photocatalytic, Optical, and Electrical Properties". ACS Nano, 2011, 5, 6726-6735.
3. Wang, Y., Liu, Y., Lu, X., Li, Z., Zhang, H., Cui, X., Zhang, Yan., Shi, F., Deng, Y., "Silver-molybdate electrocatalysts for oxygen reduction reaction in alkaline media". Electrochem. Commun., 2012, 20, 171-174
4. De Santana, Y. V. B., Ermane, J., Gomes, C., Matos, L., Cruvinel G. H., Perrin, A., Perrin, C., Andr s J., Varela, J. A., Longo, E., "Silver Molybdate and Silver Tungstate Nanocomposites with Enhanced Photoluminescence". Nanomater. Nanotechnol., 2014, 4, 22-32.
5. Bhattacharya, S., Ghosh, A., "Electrical properties of ion conducting molybdate glasses". J. Appl. Phys., 2006,100,14119-114124.
6. Prabhu, E., Muthuraja, S., Gnanasekar, K.I., Jayaraman, V., Sivabalan, S., Gnanasekaran, T., "Ammonia sensing properties of thick and thin films of $\text{Ag}_6\text{Mo}_{10}\text{O}_{33}$ and $\text{Cr}_{1.8}\text{Ti}_{0.2}\text{O}_{3+\delta}$ ". Surf. Eng., 2008, 24, 170-175.
7. Misra, S., Jayaraman, V., Gnanasekaran, T., "Trace Level Gas Sensing Characteristics of Nano-Crystalline Silver Decamolybdate". Soft. Nanosci. Lett., 2013, 3, 39-42.
8. Cui, X., Yu, S. H., Li, L., Biao, L., Li, H., Mo, M., Liu, X. M., "Selective Synthesis and Characterization of Single-Crystal Silver Molybdate/Tungstate Nanowires by a Hydrothermal Process". Chem. Eur. J., 2004, 10, 218 -223.
9. Misra, S., Sahoo, S., Jayaraman, V., Arora, A. K., Gnanasekaran, T., "Effect of annealing on microstructure and phase evolution of $\text{Ag}_6\text{Mo}_{10}\text{O}_{33}$ nanorods synthesised by novel soft chemical method". Int. J. Nanotechnol., 2010, 7, 870-882.
10. Tsilomelekis, G. and Boghosian, S., "In Situ Raman and FTIR Spectroscopy of Molybdenum(VI) Oxide Supported on Titania Combined with 18O/16O Exchange: Molecular Structure", Vibrational Properties, and Vibrational Isotope Effects. J. Phys. Chem. C., 2011, 115, 2146-2154.
11. Nakamoto, K., "Infrared Raman Spectra of Inorganic and Coordination Compounds", 6th ed., John Wiley & Sons, Inc., Hoboken, New Jersey, 2009.
12. Tadjarodi, A., Irajizad, A., Imani, M., "Mixed ammonium silver phosphomolybdate salt nanostructures; solid state synthesis, characterization of driving agent role and photocatalytic property". Mater. Lett., 2015, 161, 464-467.